HHS Public Access

Author manuscript

Sci Transl Med. Author manuscript; available in PMC 2018 September 13.

Published in final edited form as:

Sci Transl Med. 2017 September 13; 9(407): . doi:10.1126/scitranslmed.aam7621.

Peptide Probes Detect Misfolded Transthyretin Oligomers in Plasma of Hereditary Amyloidosis Patients

J. D. Schonhoft[1,2,†], **C. Monteiro**[1,2,†], **L. Plate**[1,2], **Y. S. Eisele**[1,2], **J. M. Kelly**[2], **D. Boland**[1], **C. G. Parker**[3], **B. F. Cravatt**[3], **S. Teruya**[6], **S. Helmke**[6], **M. Maurer**[6], **J. Berk**[4], **Y. Sekijima**[5], **M. Novais**[7], **T. Coelho**[7], **E. T. Powers**[1], and **J. W. Kelly**[1,2,3,*]

[1]Department of Chemistry, The Scripps Research Institute, 10550 N. Torrey Pines Road, La Jolla, CA 92037

[2]Department of Molecular Medicine, The Scripps Research Institute, 10550 N. Torrey Pines Road, La Jolla, CA 92037

[3]The Skaggs Institute for Chemical Biology, The Scripps Research Institute, 10550 N. Torrey Pines Road, La Jolla, CA 92037

[4]Boston University School of Medicine, Boston, MA 02118

[5]Department of Medicine, Neurology and Rheumatology, Shinshu University School of Medicine, Japan

[6]Columbia University College of Physicians and Surgeons, New York, NY 10032

[7]Unidade Corino de Andrade, Department of Neurosciences, Hospital de Santo António, 4099-001 Porto, Portugal

Abstract

Increasing evidence supports the hypothesis that soluble misfolded protein assemblies contribute to the degeneration of post-mitotic tissue in amyloid diseases. However, there is a dearth of reliable non-antibody based probes for selectively detecting oligomeric aggregate structures circulating in plasma or deposited in tissues, making it difficult to scrutinize this hypothesis in patients. Hence, understanding the structure-proteotoxicity relationships driving amyloid diseases remains challenging, hampering the development of early diagnostic and novel treatment strategies. Here, we report peptide-based probes that selectively label misfolded transthyretin

*To whom correspondence should be addressed: jkelly@scripps.edu; 858-784-9880.
†These authors contributed equally as co-first authors.

Author contributions: JDS, CM, JWK designed the research. JDS, CM, LP, JMK, DB performed the experiments. JDS, CM, LP, ETP, JWK analyzed the data. JDS, CM, JWK wrote the paper. CGP and BFC provided critical expertise with the diazirine photo-crosslinking experiments. YSE discovered oligomeric MTTR and provided the structural and energetic characteristics of the oligomers. ST, SH, MM, MN, JB, YS and TC provided plasma samples from patients, asymptomatic mutation carriers and controls, and clinically classified the symptomatic patients. JDS and CM contributed equally to this work.

Competing interests: JDS, CM, LP, YSE, JMK, DB, CGP, BFC, ST, SH, MM, JB, YS, MN, TC declare no competing financial interests. YS, ETP and JWK receive royalties related to tafamidis patents. JWK, JDS and CM are inventors on a patent application (Provisional patent Discl. No. 16-37; MS 29357) submitted by The Scripps Research Institute that covers the Compositions and B-peptide-based Diagnostic Methods Related to Transthyretin Amyloid Diseases.

Data and materials availability: All data is contained within the manuscript. Requests for additional information and/or reagents should be addressed to the corresponding author.

(TTR) oligomers circulating in the plasma of TTR hereditary amyloidosis patients exhibiting a predominant neuropathic phenotype. These probes revealed that there are much fewer misfolded TTR oligomers in healthy controls, in asymptomatic carriers of mutations linked to amyloid polyneuropathy, and in patients with TTR-associated cardiomyopathies. The absence of misfolded TTR oligomers in the plasma of cardiomyopathy patients suggests that the tissue tropism observed in the TTR amyloidoses is structure based. Misfolded oligomers decrease in TTR amyloid polyneuropathy patients treated with disease-modifying therapies (tafamidis or liver transplant-mediated gene therapy). In a subset of TTR amyloid polyneuropathy patients, the probes also detected a circulating TTR fragment that disappeared after tafamidis treatment. Proteomic analysis of the isolated TTR oligomers revealed a specific patient associated-signature comprised of proteins that likely associate with the circulating TTR oligomers. Quantification of plasma oligomer concentrations using peptide probes could become an early diagnostic strategy, a response-to-therapy biomarker, and a useful tool for understanding structure-proteotoxicity relationships in the TTR amyloidoses.

Introduction

Transthyretin (TTR) is a 127-amino-acid β-sheet-rich tetrameric protein that is predominantly secreted into the blood by the liver (1). Local production of TTR by the choroid plexus and the retinal epithelium accounts for the smaller quantities of TTR in the cerebrospinal fluid (CSF) (2) and the eye (3). Folded TTR circulating in blood, CSF, and in the eye of humans is known to function as a transporter of vitamin A and thyroxine (4, 5). The TTR tetramer can slowly dissociate into monomers that can subsequently misfold, enabling TTR aggregation, a process that causes proteotoxicity and ultimately the loss of post-mitotic tissue in a heterogeneous group of diseases known as the TTR amyloidoses (6–8).

Approximately 120 amyloidosis-associated TTR mutations are known (8); the autosomal dominant inheritance of one of these mutations leads to the incorporation of mutant subunits into a TTR tetramer otherwise composed of wild-type subunits, causing faster TTR tetramer dissociation kinetics and/or the accumulation of higher quantities of misfolded aggregation-prone monomers and amyloid (9). The hereditary TTR amyloidoses are systemic amyloid diseases that can present with a variety of clinical phenotypes. Patients with certain mutations, such as V122I, present predominantly with a cardiomyopathy (10), whereas other mutation carriers exhibit predominant involvement of the peripheral nervous system (11, 12), such as the V30M mutation associated with Familial Amyloid Polyneuropathy (FAP). Although the initial disease phenotype depends partially on the inherited TTR sequences (13), variability in clinical presentation is seen between patients with the same mutation and even within the same kindred, and some patients present with clinical manifestations in less commonly involved organs, such as the eye (14) (vitreous opacities and glaucoma), the central nervous system (15) (stroke and dementia) or the kidney (16) (nephrotic syndrome and chronic renal insufficiency). This poorly understood phenotypic variability or tissue tropism poses a considerable diagnostic challenge. Patients often present first to different clinical specialties with initial symptoms that mimic more common diseases, and there is currently no single diagnostic method that is non-invasive and easy to apply to diagnose the

TTR amyloidoses. Genotyping and amyloid fibril detection in tissues, combined with confirmed organ damage detected by echocardiography and/or neurophysiological assessment, are generally considered the diagnostic gold standard (17, 18). Recent cardiac imaging advances using technetium pyrophosphate show promise for the early diagnosis of the TTR amyloidoses presenting as a primary cardiomyopathy, potentially avoiding the need for invasive cardiac biopsies (19). An analogous approach is unavailable for the neurological presentation and as a direct result diagnosis is often made later in the course of disease (20). This is problematic because currently available therapeutic strategies—liver transplant-mediated gene therapy (21) or the use of pharmacologic kinetic stabilizers (tafamidis (22, 23) and diflunisal (24))—have proven to be more effective when used early in the course of FAP (25), highlighting the need for a non-invasive early diagnostic method.

(26)Although there is compelling genetic and pharmacologic evidence that the process of amyloidogenesis is the cause of the TTR amyloidoses, the mechanism(s) by which TTR aggregation or amyloidogenesis leads to organ dysfunction is not well understood (22–24). Interestingly, the insoluble cross-β-sheet amyloid fibril burden does not seem to correlate with clinical manifestations based on the observation that positive clinical responses to kinetic stabilizer therapy and/or liver transplant in TTR cardiomyopathy patients do not correlate with amyloid clearance (based on heart wall thickness measurements) (27–29). The same has been observed with disease-modifying therapies in light chain amyloidosis, another systemic amyloid disease (30, 31). Evidence from cell-based toxicity studies suggests that soluble misfolded TTR oligomers are more toxic than amyloid fibrils, although the relevance of these short-term in vitro toxicity studies to degenerative diseases that manifest over months to years remains unclear (32).

We posit that to understand aggregate structure-proteotoxicity relationships, we need to expand our knowledge about the spectrum of aggregate structures that exists in patients by developing reliable probes for each structure. The goal is to eliminate structures that do not correlate with symptom development and/or with clinical response to therapy, to produce a list of misfolded species that may drive proteotoxicity in human amyloid diseases.

Our goal was to develop probes that can selectively detect circulating non-native TTR structures that form separate from amyloid fibrils. Here we report the discovery of peptide-based probes that selectively integrate into or onto the structure(s) of non-native TTR oligomers prepared in vitro and apparently similar structures circulating in the blood of hereditary TTR amyloidosis patients with predominant neurological or mixed peripheral nervous system and cardiac phenotypes, but not in patients exhibiting primarily cardiac phenotypes. We envision that quantifying misfolded TTR oligomers in patient plasma could be useful not only for aiding physicians in point-of-care diagnosis and for following the response to particular therapies, but also for understanding the aggregate structure-proteotoxicity relationships driving the TTR amyloidoses.

Results

The B β-strand of TTR labels misfolded TTR oligomers prepared in vitro

Transthyretin forms a spectrum of aggregate structures in vitro, including amyloid fibrils (33, 34). We hypothesized that misfolded, oligomeric TTR aggregates would be less densely packed than native TTR or TTR amyloid fibrils, allowing certain peptides to integrate into such structures by docking at defect sites (Fig. 1A) not found in native TTR or in TTR amyloid fibrils, owing to their densely packed structures.

For probe discovery we used an overlapping TTR peptide library prepared by solid-phase peptide synthesis (Fig. 1B) (1). All peptides were labeled covalently at their N-termini with fluorescein. The ability of these peptides to integrate into or onto non-native TTR oligomers was assessed using oligomers prepared in vitro from a recombinant monomeric version of TTR (MTTR). MTTR harbors two mutations, one at each of the two distinct dimer interfaces (L110M, F87A), rendering MTTR unable to assemble into a native tetramer (35). Thus, MTTR aggregates readily under physiological conditions, because the slow step of tetramer dissociation has been eliminated (35). When incubated at neutral pH, MTTR undergoes conformational excursions allowing it to aggregate over a time course of a week into non-native oligomers ranging in molecular weight (MW) from 200–1000 kDa (Fig. 1C, left panel).

Each candidate peptide probe was incubated overnight with the non-native MTTR oligomers. Peptide incorporation was assayed by native polyacrylamide gel electrophoresis (PAGE) (Fig. 1C; right panel) and by size exclusion chromatography (SEC) (Figs. 1D and E). Of the 18 fluorescent peptide candidates evaluated, only the peptide derived from the B β-strand of TTR, hereafter called probe B-1, apparently incorporated into or onto the misfolded MTTR oligomers with high efficiency (Figs. 1C, D and E). The observation that probe B-1 remains bound after SEC suggests that the probe-oligomer complex has a very slow dissociation rate.

The same approach assessed whether probe B-1 incorporated into TTR oligomers made from $TTR_{50–127}$, which lacks the B β-strand (fig. S1A). This TTR fragment is found in biopsies of cardiomyopathy and some polyneuropathy patients (36). Again probe B-1 was the only peptide of 18 that incorporates into $TTR_{50–127}$ oligomers (fig. S1B).

B-1 integrates into or onto a cross-β-sheet structure

An alanine scan across the probe B-1 sequence revealed that every other residue was important for its incorporation into misfolded TTR oligomers (underlined residues in Fig. 1F). The apparent requirement for every other residue being a β-branched amino acid is consistent with probe B-1 binding to or integrating into a cross-β-sheet structure harboring a defect site or onto a protofilament end (Fig. 1A) (37, 38). Truncation of probe B-1 from the N- and C-termini identified the sequence *VAVHVF* as the minimal binding competent sequence, although the truncated peptide incorporated to a much lesser extent (90% less) compared to probe B-1(fig. S2).

Probe B-1 is selective for nascently formed non-native TTR oligomers

After incubating probe B-1 with natively folded WT TTR tetramers, or freshly purified homotetramers comprising disease-associated TTR subunits (V30M, L55P, V122I, T60A, A25T TTR) or the interallelic stabilizing mutation (T119M) (9), minimal labeling of the tetramer was observed (Fig. 2A; right panel), indicating that probe B-1 is selective for non-native aggregate structures over densely side-chain-packed natively folded tetrameric TTR. The highly destabilized A25T TTR tetramer readily dissociates and the resulting monomers misfold and misassemble under physiological conditions, forming high MW oligomers within 24 h (39). Probe B-1 intensely labeled these non-native TTR oligomeric aggregates (Fig. 2A, right panel). After correction for fluorescence quenching (fig. S3), we found that MTTR oligomers undergoing active aggregation more readily incorporated probe B-1 than MTTR that had been oligomerizing for more than 15 days (Fig. 2B). Probe B-1 incorporated into nascent oligomers in a stoichiometry of ≈ 1:1 B-1:MTTR monomer (fig. S3). Our results suggest that a fundamental structural commonality exists between the MTTR, $TTR_{50–127}$ and A25T non-native TTR oligomers that allows probe B-1 binding. This structural motif is not present in native TTR tetramers or folded MTTR.

To test whether probe B-1 incorporates into TTR amyloid fibrils, we stained salivary gland biopsies of a V30M FAP patient and a healthy control with a biotin labeled version of probe B-1 (B-1-Biotin). As expected (40), amyloid fibrils in the salivary gland were localized around glandular acini as revealed by thioflavin T fluorescence (Fig. 2C top left panel, white arrows, and fig. S4), an amyloid selective fluorophore. An anti-TTR antibody confirmed these are TTR-derived amyloid fibrils (Fig. 2C, third row of left panels). Probe B-1-Biotin was found inside the glandular acini of both patient and control (Fig. 2C, white asterisks, **and** fig. S4), revealing that the peptide does not bind to or integrate into or onto TTR amyloid fibrils present within tissue, instead it is non-specifically binding to something inside the glandular cells.

Probe B-1 selectively differentiates FAP patient samples from controls

Native PAGE and SEC were employed to discern whether probe B-1 could label exogenous MTTR oligomers that were added to the plasma of a healthy donor. Probe B-1 selectively labeled the non-native MTTR oligomers and exhibited a linear SEC response with misfolded oligomeric TTR concentration (fig. S5). Notably, an Ala-scan structure-activity relationship (SAR) with probe B-1 analogs added to plasma containing non-native MTTR oligomers (fig. S6) was similar to that observed with non-native MTTR oligomers in buffer (Fig. 1F), addressing selectivity even in this complex biological fluid.

Probe B-1 was incubated with plasma from symptomatic Portuguese and Japanese V30M FAP patients, asymptomatic Portuguese V30M mutation carriers, and healthy controls. All patients had symptoms defining disease onset at the time the blood samples were collected and most patients had a neurological impairment score of the lower limbs (NIS-LL) of less than 10 points, reflecting early stage FAP (25). By both SEC and native PAGE analyses, probe B-1 labeled the high MW fraction from the FAP patients (Fig. 3A and B). In contrast, only minimal labeling was observed in the control groups. In a larger cohort, analysis of plasma showed a statistically significant increase in the high MW fluorescence SEC peak

eluting between 800–1200 μL in the FAP patients relative to the control groups (Fig. 3C, $P < 0.0001$). Similar results were obtained using a B-peptide wherein the fluorescein substructure is replaced by disulfoCy5, showing that use of a less environmentally sensitive fluorophore makes no difference (fig. S7).

The SAR of the probe B-1 alanine mutants with V30M FAP patient plasma showed the same trend as when the probe B-1 alanine mutants were added to control plasma to which MTTR oligomers were added (fig. S8). Substitution of any of the core β-branched amino acids eliminated the fluorescence intensity of the 800–1200 μL SEC peak. We also reevaluated TTR-based peptide probes from the eight β-strands (Fig. 1B) using FAP patient plasma and only probe B-1 exhibited fluorescent intensity in the high MW gel filtration peak (800–1200 μL; fig. S9). Collectively, these results suggest that probe B-1 recognizes circulating misfolded TTR oligomers in patients that have not been detected previously.

Diazirine photo-crosslinking probe B-2 validates the identification of non-native TTR oligomers

To distinguish between probe B-1 binding to naked non-native TTR oligomers in FAP patient plasma versus non-native TTR oligomers interacting with holdase chaperones, like clusterin, and potentially other plasma proteins, we incorporated a diazirine functional group and an alkyne handle into probe B-1, generating probe B-2 (Fig. 4A). Upon irradiation at 355 nm, the diazirine forms a highly reactive short-lived (~100 ns) carbene that inserts into proximal bonds, resulting in covalent conjugates with the target protein(s) and potentially other macromolecules (41, 42). After incubation of probe B-2 with plasma samples, the samples were irradiated and rhodamine-azide was covalently attached to the alkyne handle using a protein denaturing copper catalyzed alkyne-azide cycloaddition (CuAAC) or ‘click’ reaction to render the conjugates fluorescent. Denaturing and reducing SDS PAGE was used to identify proteins comprising the fluorescently labeled conjugates, including initially aggregated non-native TTR (Fig. 4B).(43, 44)

As a positive control, we showed that probe B-2 selectively labeled MTTR oligomers, both in buffer (fig. S10) and when oligomers were added to the plasma of healthy donors, but did not label natively folded tetrameric TTR also present in μM concentrations within plasma (Fig. 4C, middle panel, magenta box; note the absence of signal in lane 1 and the presence of signal in lane 2 (MTTR oligomers added)). Thus probe B-2 displayed a high degree of selectivity for non-native TTR oligomers. Control experiments with peptide probe B-2C, lacking the diazirine, exhibited minimal TTR oligomer labeling (Fig 4C; middle panel, lanes 3 and 4), indicating that labeling is dependent on the presence of the diazirine cross-linker, facilitating fluorescence-based detection and analysis of the denaturing SDS-PAGE separation.

Probe B-2 was incubated with FAP patient plasma (recall these samples exhibited the high MW SEC fluorescence signal upon incubation with probe B-1). After photo-crosslinking and rhodamine conjugation, a band that migrates equally to that of monomeric TTR (13.5 kDa) was covalently labeled by probe B-2 in the denaturing SDS-PAGE analysis of FAP patient plasma, but minimally in the plasma from a healthy donor (Fig. 4D, middle panel, magenta box), again demonstrating that probe B-2 does not form a complex with the

natively folded TTR tetramer prior to photo-crosslinking. Notably, the SDS-PAGE readout revealed that other higher MW proteins are labeled by probe B-2 differentially between patients and controls (Fig. 4D, middle panel).

To identify the proteins present in the high MW SEC fractions, representative plasma samples were incubated with probe B-2, photo-crosslinked, and subjected to non-denaturing SEC fractionation prior to performing a proteome denaturing rhodamine click reaction on each chromatographic fraction. These samples were then subjected to denaturing SDS-PAGE (Fig. 4E summarizes workflow). In V30M FAP plasma, TTR was present in the high MW SEC fractions (3–5; 800–1200 μL) (Fig. 4F, middle panel, magenta box). TTR, observed as a monomer in SDS PAGE in the rhodamine channel, was in a more than 200 kDa MW complex, because only TTR in the "high MW fractions" (3–5) reacted with covalent probe B-2. In contrast, a healthy donor plasma sample incubated with probe B-2 and irradiated did not crosslink with native WT TTR (Fig. 4F; right side middle panel), despite evidence that TTR was present in many fractions (Fig. 4F, bottom panel, dark green box). Thus, probe B-2 only photo-conjugates high MW non-native TTR oligomers in the patient plasma and not native TTR in healthy donor plasma, demonstrating its selectivity.

The intensity of the B-2-TTR SDS-PAGE conjugate band from the high MW fraction was quantified by densitometry in a larger set of V30M FAP patients, asymptomatic V30M carriers, and healthy donor controls. Significantly more non-native TTR was labeled in the V30M FAP patient group compared with healthy donors and asymptomatic V30M mutation carriers (Fig. 4G & fig. S11; Table 1, $P < 0.0001$, $P = 0.0004$, respectively). Probe B-2 plasma protein conjugates from the high MW fraction were subjected to a click reaction with biotin, and subsequently the probe B-2 crosslinked proteins were affinity purified from patient and control plasma. TTR was identified in the eluted fractions by SDS-PAGE visualized by anti-TTR western blot—non-native TTR was found to be more prominent in the patient samples (Fig. 4H). Control experiments showed that the B-peptide sequence itself does not cross-react with the anti-TTR antibody used, thus the anti-TTR antibody is recognizing an antigen other than the B-peptide sequence (fig. S12).

Quantitative proteomics identifies the targets of the B-2 probe beyond non-native TTR oligomers

Unbiased proteomics experiments were performed to compare the relative abundances of the probe B-2 target protein conjugates in plasma samples from 3 Portuguese V30M FAP patients, 3 Portuguese asymptomatic V30M carriers, and 3 healthy donors (Fig. 5A summarizes the workflow). Probe B-2 was incubated with the plasma samples overnight, photo-crosslinked and the conjugates were affinity purified by clicking on biotin to the alkyne handle. An identical diazirine and alkyne containing B peptide analog harboring a single alanine substitution (B-2-Mut, AIN**A**AVHVFR, V28A) to eliminate labeling of MTTR oligomers (Fig. 1F, fig. S6 and S8) was used as a control probe. Rhodamine gel labeling experiments confirmed that probe B-2-Mut does not label non-native TTR oligomers in FAP patients (Fig. 5B, rightmost panel, magenta box). After affinity purification, each sample was digested with trypsin, and the tryptic fragments were labeled by one of six unique isobaric mass tags (TMT tags are amine reactive) (45). The 6 samples

(3 unique V30M FAP patient samples treated with B-2 or B-2-Mut) were then combined and subjected to multidimensional protein identification technology liquid chromatography-mass spectrometry/mass spectrometry (MudPIT LC-MS/MS) analysis and the relative abundances of the tryptic peptides in each of the six samples were quantified by the intensity of the unique fragments in the MS2 spectra. Proteins of interest were expected to be labeled by probe B-2, but not the probe B-2-Mut; in other words, the intensity of the identified peptides in the MS2 spectra was expected to be higher in the probe B-2 treated TMT channels, relative to the probe B-2-Mut TMT channels.

In the FAP data set, 99 unique proteins were identified by the affinity purification mass spectrometry approach (Fig. 5C). The highest intensity protein was serum albumin, as expected because it binds the hydrophobic peptide probe B-2 and is the most abundant protein in human plasma (table S1). For the high abundance plasma proteins, the spectral counts of the identified proteins correlated with their expected plasma concentration (fig. S13). However, sorting the protein list by the intensity ratio of probe B-2 to probe B-2-Mut, the most "B-2 enriched" proteins were TTR, several apolipoproteins [including apoE (36 kDa)], clusterin (CLU; 37 kDa), vitronectin (VTN; 75 kDa), Cadherin-5 (CDH5; 90 kDa), Complement C1s (C1S; 86 kDa) and alpha-2-macroglobin (A2M; 180 kDa) (Fig. 5D and E). Notably, the majority of the proteins that are most confidently identified by proteomics here have been previously found in amyloid tissue biopsies from FAP patients, suggesting that these proteins may circulate with non-native TTR oligomers.

A clear proteomic signature emerged that distinguished FAP patients from healthy donors and asymptomatic carriers. The majority of probe B-2 targets identified in the FAP patients were also identified, including TTR, in the controls (Fig. 5C). The enrichment ratio for TTR was greatest for FAP patients, lesser for asymptomatic carriers, and least in healthy controls exhibiting no enrichment (probe B-2: probe B-2-Mut ~ 1) (Fig. 5F). In contrast, the ratios for the circulating interacting proteins, namely clusterin (a holdase chaperone), apoE (transports lipoproteins, fat soluble vitamins and cholesterol), and vitronectin (functions in hemostasis and modulating cell adhesion), displayed an inverse trend where the probe B-2: probe B-2-Mut ratio was lowest for the FAP patients (Fig. 5F). The biochemical and proteomics experiments described thus far fully validate non-native oligomeric TTR as a clear target of the B-2 probe, along with several TTR associated proteins that may also be bound to TTR oligomers.

Misfolded TTR oligomer quantities decrease in FAP plasma upon treatment

Tafamidis is a transthyretin kinetic stabilizer that is approved for use in 37 countries to ameliorate FAP. Tafamidis slows FAP progression based on placebo-controlled clinical trial data (22, 23). We used covalent probe B-2 to analyze the concentration of non-native TTR oligomers in the plasma of 15 Portuguese V30M FAP patients at the time of diagnosis and after 12 months of tafamidis (20 mg daily) administration (average NIS-LL change = −0.1). The majority of these patients were diagnosed early in the course of the disease with NIS-LL scores of ≤10 and are considered to be clinical responders (annual progression of NIS < 2 points) (46). Labeling of non-native TTR in the high MW SEC fraction by probe B-2 was reduced or unchanged in 12 of 15 patients, and increased in 3 patients (Fig. 6A and B). In

the 15 patients analyzed, non-native TTR labeling decreased on average by 1.8 fold after 12 mo of tafamidis treatment.

We also tested 7 Japanese V30M FAP patients who had undergone liver transplant-mediated gene therapy several years earlier, eliminating the presence of the V30M protein in the circulatory system and slowing the progression of FAP (21). In these samples, no detectable non-native TTR was observed (Fig. 6C).

Circulating proteolyzed TTR is identified in some FAP patient plasma samples

In a few FAP pre-tafamidis plasma samples incubated with covalent probe B-2, labeling of a lower MW TTR band (~9–10 kDa) was observed in the high MW SEC fraction (patients 5, 6 and 7. Importantly, fragmented TTR was not present in patients 5–7 after 12 mo of tafamidis treatment (Fig. 6A and fig. S14A). This fragment is slightly larger than the expected molecular weight of the C-terminal TTR fragment ($TTR_{50–127}$, 8666 Da) found to comprise amyloid fibrils deposited in a subset of TTR cardiomyopathy patients (36, 47). We further probed all 15 of these patient plasma samples by western blot using a C-terminus-specific TTR antibody (fig. S14B). In samples from patients 5, 6 and 7, a band was observed at approximately 9–10 kDa in SDS-PAGE by western blot analysis, indicating that this band was a TTR fragment. Control experiments in which a protease inhibitor cocktail was added immediately after thawing the plasma samples showed no difference in the intensity of the TTR cleavage band, demonstrating that active proteolysis during peptide probe incubation is likely not responsible for the observed TTR proteolysis (fig. S14C). Collectively, the data outlined in Fig. 6 and fig. S14 suggest that C-terminally proteolyzed TTR is circulating in the blood of a subset of FAP patients.

Non-native TTR is detected in polyneuropathy-selective genotypes but not in cardiomyopathy-selective genotypes

Further scrutiny of whether covalent probe B-2 can detect non-native TTR oligomers in plasma of genotypes other than those harboring the V30M FAP mutation was undertaken (Fig. 7, V30M data shown in Fig. 4G is presented again to facilitate comparisons). We tested plasma samples from 32 additional patients (15 WT-cardiomyopathy, 6 V122I cardiomyopathy, 4 T60A mixed polyneuropathy and cardiomyopathy, and 7 other mutations associated with TTR amyloidosis) (Table 1, Fig. 7). We observed a trend wherein non-native oligomeric TTR was readily detectable in genotypes associated with a primary neuropathic phenotype, but not in genotypes associated with a primary cardiomyopathy phenotype (WT, V122I) (Fig. 7). Finally, although requiring many assumptions, we estimated the concentration of these oligomers to be in the low nM range in ployneuropathy plasma based on monomer concentration (SI: Estimation of Non-Native TTR in Patient Plasma).

Discussion

We have developed peptide probes that selectively recognize non-native TTR oligomers circulating in the plasma of hereditary TTR amyloidosis patients exhibiting a predominant polyneuropathy phenotype. Our probe B-2 photo-crosslinks to non-native TTR in oligomers, allowing us to isolate oligomers from patient plasma as well as the proteins that likely

interact with the oligomers. This covalent probe also revealed that fragmented TTR circulates in the high molecular weight fraction in the plasma of a subset of polyneuropathy patients. Importantly, non-native TTR oligomer concentrations decrease upon disease-modifying treatments, suggesting that the structure-proteotoxicity relationship of these oligomers should be further scrutinized.

A limitation of our study is that we lack a detailed structural understanding of how our probes bind to non-native TTR oligomers. Furthermore, we were unable to test whether a correlation exists between oligomer concentration and disease severity owing to the small number of patients evaluated.

An advantage of the peptide-based probes introduced here is that, unlike other amyloid-selective probes used for diagnostic purposes such as Congo Red or thioflavin T, our probe preferentially recognizes soluble, misfolded and actively aggregating TTR oligomers that adopt a non-amyloid quaternary structure. Because the probes detect non-native TTR in early stage neuropathic TTR amyloidosis patients (NIS-LL < 10), they may be suitable for detection of early events that lead to degenerative phenotypes, that is, useful for early diagnosis. Peptide-based probes for soluble amyloid β oligomers have been developed by other groups and exhibit oligomer selectivity; however their utility has not yet been tested in patients (48–50).

The selectivity of covalent peptide probe B-2 for non-native TTR oligomers may prove to be useful as a response-to-therapy biomarker, as treatments that slow the progression of polyneuropathy (tafamidis treatment or liver transplant-mediated gene therapy) significantly lower non-native TTR oligomer concentration. Either probe B-1 or probe B-2 could be elaborated beyond the lower-throughput methods used in this paper, for example by conversion to an ELISA format, more commonly used by clinical laboratories, rendering these peptide probes more generally useful.

Non-native TTR has the highest MS enrichment ratio in FAP patients, whereas the enrichment ratio for apoE and clusterin is lowest in FAP patients. One hypothesis is that the non-native TTR oligomers are titrating our probes away from apoE and clusterin.

Probe B-2 was able to identify circulating fragmented TTR in a subset of polyneuropathy patients. In a histopathological study of FAP and WT TTR cardiomyopathy patients, Westermark and colleagues (36, 47) showed that C-terminally cleaved TTR was identified in all WT TTR cardiac amyloid fibril biopsies, whereas a mixture of cleaved and full-length TTR was detected in the amyloid fibrils extracted from the tissue of FAP patients. Our data suggest that TTR is cleaved prior to deposition and after rate-limiting dissociation of the native tetramer, as tafamidis treatment stops the aberrant endoproteolysis presumably by kinetically stabilizing the native tetramer. Aberrant endoproteolysis of the monomer could change the structure of the TTR aggregates that are formed, leading to unique proteotoxicity mechanisms and potentially explaining why there is early onset versus late onset V30M FAP, or why FAP in males typically progresses faster than in women (51, 52).

Our probes generate data that allow us to begin to think about what is responsible for the tissue tropism exhibited by the TTR amyloidoses. A one amino acid change in the TTR

sequence determines whether non-native TTR oligomers are detected in patient plasma by our probes. That probe B-2 is unable to detect circulating non-native TTR oligomers in the plasma of cardiomyopathy patients (Fig. 7; WT or WT and specific TTR mutants aggregating) suggests that a unique aggregate structure enabling rapid heart deposition may be a determinant for the cardiomyopathy phenotype. Evidence from other amyloid diseases indicates that conformational differences between aggregates may be responsible for distinct disease etiologies (53, 54).

Materials and Methods

Study Design

The objective of this study was to develop peptide-based probes that recognize transthyretin oligomers and to show their utility in detection of oligomers in the plasma of patients with hereditary amyloidosis. All patient samples and analyses were collected under the approved IRB protocols at their respective institutions and no blinding or randomization was used. The number of unique clinical plasma samples for each experiment is indicated in the respective figures and legends. We chose plasma from healthy blood donors and asymptomatic mutation carriers as controls. Sample sizes in the range of 10–50 were chosen for feasibility in accrual and provided a reasonable degree of statistical power for comparison of the three groups.

Peptide synthesis and purification

Resin was purchased from Millipore-Sigma (NovaSyn TGR, cat# 855009) and amino acids used for peptide synthesis were purchased from Novabiochem Corp. HOBt (1-hydroxy-benzotriazole; Advanced Chem Tech), HBTU (hexafluorophosphate; Anaspec), DIEA (N,N-diisopropylethylamine, Applied Biosystems) were used as coupling reagents and piperidine (Sigma Aldrich) was used for the standard deprotection method. The peptides were cleaved from the resin using 87.5: 5: 5: 2.5; trifluoroacetic acid, thianisole, water, 1,2-ethanedithiol. Peptides were synthesized on an Applied Biosystems 433A automated peptide synthesizer using a standard FMOC protection strategy. Typically after synthesis, the cleaved peptide was precipitated using cold diethylether, recovered by centrifugation, reconstituted in anhydrous DMF or DMSO and incubated with 5-FAM-X-SE (6 - (Fluorescein - 5 - carboxamido)hexanoic acid, succinimidyl ester, Anaspec Inc), or SE-PEG2 Biotin (Broadpharm) or SE-Diazirine (ThermoFisher Scientific, ‘SDA’ (NHS-Diazirine cat# 26167)) for two hours in the presence of DIEA (1:100 DIEA/DMF). For sequences that contain lysine, fluorophore coupling was done on the resin prior to deprotection and cleavage. Purification of labeled peptides was achieved using preparative C18 RP-HPLC (Buffer A: 0.1% TFA in water, Buffer B: 0.1% TFA in acetonitrile). Peptides masses were confirmed by LC-MS. After purification the fractions containing the peptide of interest were lyophilized and stored under dessicant at −20 °C. Prior to each experiment peptides were freshly reconstituted in DMSO for use.

Expression and purification of recombinant TTR

Recombinant wild-type, mutant TTR (MTTR corresponding to F87M/L110M TTR mutant, A25T, V30M, L55P, T119M, V122I, T60A) and C-terminal TTR fragment ($TTR_{50–127}$)

were expressed and purified from *E. coli* as described previously (34). Detailed information can be found in the supplementary methods.

Production of non-native recombinant TTR oligomers and aggregates and SEC analysis of peptide incorporation

A25T TTR and MTTR readily form stable oligomers at neutral pH. Briefly, as previously described (34, 35, 39), the proteins were concentrated to 2 mg/mL in 10 mM sodium phosphate pH 7.6, 100 mM KCl, 1 mM EDTA and incubated at 37 °C as indicated. To make aggregates of $TTR_{50–127}$, 0.5 mg of the lyophilized powder was dissolved in 10 mM sodium phosphate pH 7.6, 100 mM KCl, 1 mM EDTA to a final concentration of 70 μM. The solution was placed in sonicating water bath for 5 minutes to fully dissolve the peptide and then passed through a 0.2 μm filter and incubated at room temperature for 4 hours. Details relating to the peptide screen and stoichiometry experiments are in the Supplementary Materials.

Salivary gland biopsies staining with thioflavin T, anti-TTR antibody and B-1-Biotin

Serial sections of formalin-fixed and paraffin-embedded salivary gland biopsies from FAP V30M symptomatic patients (n=2) and non-FAP controls (n=2) were obtained. Sections (4 per sample) were deparaffinized, re-hydrated, and stained with thioflavin T, anti-TTR antibody or B-1-Biotin probe. All slices were visualized using an Olympus IX71 Inverted Microscope. Low magnification images (5x) including most of the tissue on each section were taken (1–2 photos/section) and 1–2 images of selected areas/slice were taken using the 20x magnification. All images were acquired using an attached microscope camera Hamamatsu C8484-03G01 and the HCImage software.

Incubation of plasma samples with probe B-1 and size exclusion chromatography

Plasma (45 μL) was incubated with probe B-1 (20 μM; 3.2 μL of probe B-1 from a 300 μM stock solution in DMSO) or 3.2 μL of DMSO for 24 hours at 37°C. Before injecting onto the size exclusion column (Acquity UPLC protein BEH SEC Column, 200Å, 1.7 μm, 4.6 mm × 150 mm, Waters), each plasma sample was filtered through a P30 gel filtration column (Bio-Spin Columns with Bio-Gel P-30) to remove excess unbound peptide and preserve the lifespan of the SEC column (final volume = 50 μL). 5 μL of each sample was then injected onto the column and separated using a constant flow of 0.2 mL/min of 10 mM phosphate buffer, 1 mM EDTA, 100 mM KCl, pH 7.8, for 30 minutes. To account for plasma auto-fluorescence, the resulting signal from the samples with no probe B-1 (DMSO only) was subtracted from the signal from the corresponding sample with the probe B-1. At the start and the end of each sample set, four injections of different concentrations of fluorescein in the running buffer (freshly prepared each day) were analyzed by the same instrument, in order to make a standard curve for day-to-day comparison. All data were then normalized to the total protein concentration as calculated from the integrated area in the 280 nm absorbance channel. The results of the three groups were compared using a one-way analysis of variance (ANOVA) test.

Diazirine photo-crosslinking and pulldown

Lyophilized probe B-2 powder was weighed and dissolved in DMSO to a final stock concentration of 1 mM and added to the plasma samples to give a final concentration of 50 μM and incubated at 37°C overnight. Time course experiments with plasma from patients and MTTR oligomers within plasma from healthy donors, showed that the signal plateaued within 5–8 hours and did not change thereafter. After incubation, plasma was pipetted into a 96-well plate with a non-binding surface (Corning #3650) and irradiated at 355 nm in a Stratalinker UV Crosslinker 1800 for 1 hour. After photo-activation and crosslinking, free peptide was removed and the probe B-2 conjugates buffer exchanged into 10 mM sodium phosphate buffer (pH 7.6), 100 mM KCl using a spin gel filtration column (Bio-Spin Columns with Bio-Gel P-30). 5–20 μL of the sample was then injected onto a Acquity UPLC Protein BEH SEC Column, 200Å, 1.7 μm, 4.6 × 150 mm, Waters or an Agilent Bio SEC-3 4.6 × 300 mm size exclusion column [mobile phase 10 mM sodium phosphate buffer (pH 7.6), 100 mM KCl]. Both columns separate biomolecules in the range of 100–600 kDa; the Agilent Bio SEC-3 has a higher loading capacity and was used specifically for this reason for quantification of non-native TTR in Fig. 4F, Fig. 6 and Fig. 7. Aliquots of the samples either before or after SEC were conjugated with either Rhodamine-azide (tetramethylrhodamine azide, cat# 7130 Lumiprobe) or Diazo-Biotin-azide (cat# BP-22477, BroadPharm) using the copper catalyzed click reaction (55, 56). For the click reaction, per 50 μL of sample, 1 μL of 5 mM azide containing probe (100 μM) was added to the sample and mixed, followed by the addition of 5 μL a 50:50 mix of 1 M $CuSO_4$ and BTTP ligand. The reaction was then initiated by addition of 1 μL of sodium ascorbate (20 mg/mL in water) and incubated at 30°C for 1 hour with gentle mixing.(56)

Quantitative Proteomics using TMT isobaric mass tags

Plasma samples from 3 unique individuals were run in parallel using the following scheme. Plasma (95 μL) was mixed with 5 μL of either probe B-2 or probe B-2-Mut and incubated and crosslinked as described above. The plasma samples were then passed through a Bio-Spin P-30 gel-filtration column equilibrated in 10 mM phosphate buffer pH 7.6, 100 mM KCl and subjected to conjugation of N_3-Diazo-Biotin as described above. Probe-crosslinked proteins were enriched using streptavidin agarose as described above. The biotin-enriched eluted protein samples were then precipitated in methanol/chloroform and washed twice with 100% methanol. The air-dried protein pellets were then resuspended, reduced, acetylated and trypsin digested, and labeled with respective TMT-NHS isobaric reagents (Thermo Fisher) as described previously (57). The 3 plasma samples treated with either probe B-2 or probe B-2-mut were pooled, resulting in a total of 6 channels per run. MudPIT columns were prepared as described previously (57) and LC-MS/MS analysis was performed using a Q-Exactive mass spectrometer with an EASY nLC 1000 (Thermo) LC pump. MudPIT experiments consisted of 5 min sequential injections of 0, 20, 50, 80, 100 % buffer C (500 mM ammonium acetate in buffer A) followed by a final step of 10 % buffer B (20% water, 80% acetonitrile, 0.1% formic acid v/v/v)/90% buffer C (95% water, 5% acetonitrile, 0.1% formic acid, v/v/v). Each injection was followed by a linear gradient from buffer A (95% water, 5% acetonitrile, 0.1% formic acid, v/v/v) to buffer B. Electrospray was carried out directly from the analytical C18 columns by applying a voltage of 2.5kV using an inlet capillary temperature of 275°C. Data-dependent acquisition of MS/MS spectra was

performed as described before (57). Protein identification and quantification of TMT labeling intensities was carried out using the Integrated Proteomics Pipeline Suite (IP2, Integrated Proteomics Applications, Inc.,) as described previously (57). Global normalization of TMT intensities across the 6 channels was carried out within Census in IP2. Enrichment of a protein in the probe B-2–treated samples versus probe B-2-Mut–treated samples was calculated as the difference in log2 combined TMT intensities of the protein for a given patient.

Statistical Analysis

All graphs and statistics were prepared in Prism 6 (Graphpad Software). For binary comparisons, a two-tailed t-test assuming equal standard deviations was used. For comparisons between three or more groups, we used ANOVA test followed by post-hoc analysis with Tukey correction for multiple pairwise comparisons. For LC MS/MS data, enrichment differences (B-2 versus B-2-Mut) were averaged across the 3 patients and significance was tested using unpaired t-tests assuming equal standard deviations across sample populations, followed by a multiple testing correction using a two-stage linear step-up procedure (58) and a desired FDR of 5% (table S1). All *P*-values are marked in the legends and figures. All box plots represent the mean and first and third quartile and values. All values are expressed as the mean ± one standard deviation. All raw data for experiments where N < 20 are reported in table S2.

Supplementary Material

Refer to Web version on PubMed Central for supplementary material.

Acknowledgments

We thank Dr. Xin Jiang and Dr. Justin Chapman from Misfolding Diagnostics, Inc, for supplying biotin-labeled anti-TTR antibody (DAKO) and Dr. Per Westermark for the monoclonal C-terminal TTR antiserum. We thank Dr. Manuel Melo Pires, Dr. Ricardo Taipa and Inês Reis for providing salivary gland biopsy sections and technical support with the results interpretation.

Funding: This work was supported by the Skaggs Institute for Chemical Biology and by National Institutes of Health grants DK046335 and UL1TR001114 (JWK), and CA132630 (BFC). JDS was supported by a Damon Runyon Postdoctoral Fellowship (DRG-2230-15), CM by an American Heart Association Predoctoral Grant 16PRE31130009 and LP by a fellowship from the Leukemia and Lymphoma Society. YSE was supported by a fellowship from the German Academic Exchange Service, (DAAD), and by a K99 award by the National Institute on Aging (1K99 AG050764). CGP was supported by a postdoctoral fellowship (PF-14-100-01-CDD) from the American Cancer Society. JB was funded by the Young Family Amyloidosis Research Fund.

References

1. Blake CC, Geisow MJ, Oatley SJ, Rerat B, Rerat C. Structure of prealbumin: secondary, tertiary and quaternary interactions determined by Fourier refinement at 1.8 A. J Mol Biol. 1978; 121:339–356. [PubMed: 671542]
2. Herbert J, Wilcox JN, Pham KT, Fremeau RT Jr, Zeviani M, Dwork A, Soprano DR, Makover A, Goodman DS, Zimmerman EA, et al. Transthyretin: a choroid plexus-specific transport protein in human brain. The 1986 S. Weir Mitchell award. Neurology. 1986; 36:900–911. [PubMed: 3714052]
3. Cavallaro T, Martone RL, Dwork AJ, Schon EA, Herbert J. The retinal pigment epithelium is the unique site of transthyretin synthesis in the rat eye. Invest Ophthalmol Vis Sci. 1990; 31:497–501. [PubMed: 1690688]

4. Monaco HL, Rizzi M, Coda A. Structure of a complex of two plasma proteins: transthyretin and retinol-binding protein. Science. 1995; 268:1039–1041. [PubMed: 7754382]

5. Hagen GA, Elliott WJ. Transport of thyroid hormones in serum and cerebrospinal fluid. J Clin Endocrinol Metab. 1973; 37:415–422. [PubMed: 4206491]

6. Colon W, Kelly JW. Partial denaturation of transthyretin is sufficient for amyloid fibril formation in vitro. Biochemistry. 1992; 31:8654–8660. [PubMed: 1390650]

7. Lai Z, Colon W, Kelly JW. The acid-mediated denaturation pathway of transthyretin yields a conformational intermediate that can self-assemble into amyloid. Biochemistry. 1996; 35:6470–6482. [PubMed: 8639594]

8. Sekijima Y. Transthyretin (ATTR) amyloidosis: clinical spectrum, molecular pathogenesis and disease-modifying treatments. J Neurol Neurosurg Psychiatry. 2015; 86:1036–1043. [PubMed: 25604431]

9. Hammarstrom P, Schneider F, Kelly JW. Trans-suppression of misfolding in an amyloid disease. Science. 2001; 293:2459–2462. [PubMed: 11577236]

10. Ruberg FL, Berk JL. Transthyretin (TTR) cardiac amyloidosis. Circulation. 2012; 126:1286–1300. [PubMed: 22949539]

11. Plante-Bordeneuve V, Said G. Familial amyloid polyneuropathy. Lancet Neurol. 2011; 10:1086–1097. [PubMed: 22094129]

12. Andrade C. A peculiar form of peripheral neuropathy; familiar atypical generalized amyloidosis with special involvement of the peripheral nerves. Brain. 1952; 75:408–427. [PubMed: 12978172]

13. Zeldenrust SR. Genotype--phenotype correlation in FAP. Amyloid. 2012; 19(Suppl 1):22–24. [PubMed: 22620962]

14. Seca M, Ferreira N, Coelho T. Vitreous Amyloidosis as the Presenting Symptom of Familial Amyloid Polyneuropathy TTR Val30Met in a Portuguese Patient. Case Rep Ophthalmol. 2014; 5:92–97. [PubMed: 24748873]

15. Herrick MK, DeBruyne K, Horoupian DS, Skare J, Vanefsky MA, Ong T. Massive leptomeningeal amyloidosis associated with a Val30Met transthyretin gene. Neurology. 1996; 47:988–992. [PubMed: 8857732]

16. Lobato L, Rocha A. Transthyretin Amyloidosis and the Kidney. Clin J Amer Soc Nephrol. 2012; 7:1337–1346. [PubMed: 22537653]

17. Ando Y, Coelho T, Berk JL, Cruz MW, Ericzon BG, Ikeda S, Lewis WD, Obici L, Plante-Bordeneuve V, Rapezzi C, Said G, Salvi F. Guideline of transthyretin-related hereditary amyloidosis for clinicians. Orphanet J Rare Dis. 2013; 8:31. [PubMed: 23425518]

18. Obici L, Kuks JB, Buades J, Adams D, Suhr OB, Coelho T, Kyriakides T. Recommendations for presymptomatic genetic testing and management of individuals at risk for hereditary transthyretin amyloidosis. Curr Opin Neurol. 2016; 29(Suppl 1):S27–35. [PubMed: 26734953]

19. Gillmore JD, Maurer MS, Falk RH, Merlini G, Damy T, Dispenzieri A, Wechalekar AD, Berk JL, Quarta CC, Grogan M, Lachmann HJ, Bokhari S, Castano A, Dorbala S, Johnson GB, Glaudemans AW, Rezk T, Fontana M, Palladini G, Milani P, Guidalotti PL, Flatman K, Lane T, Vonberg FW, Whelan CJ, Moon JC, Ruberg FL, Miller EJ, Hutt DF, Hazenberg BP, Rapezzi C, Hawkins PN. Nonbiopsy Diagnosis of Cardiac Transthyretin Amyloidosis. Circulation. 2016; 133:2404–2412. [PubMed: 27143678]

20. Plante-Bordeneuve V, Ferreira A, Lalu T, Zaros C, Lacroix C, Adams D, Said G. Diagnostic pitfalls in sporadic transthyretin familial amyloid polyneuropathy (TTR-FAP). Neurology. 2007; 69:693–698. [PubMed: 17698792]

21. Benson MD. Liver transplantation and transthyretin amyloidosis. Muscle Nerve. 2013; 47:157–162. [PubMed: 23169427]

22. Coelho T, Maia LF, Martins dSA, Waddington CM, Plante-Bordeneuve V, Lozeron P, Suhr OB, Campistol JM, Conceicao IM, Schmidt HHJ, Trigo P, Kelly JW, Labaudiniere R, Chan J, Packman J, Wilson A, Grogan DR, Imventarza OC, Wainberg PJ, Berra LM, Maultasch H, Gold J, Bardera JCP, Zibert A. Tafamidis for transthyretin familial amyloid polyneuropathy: A randomized, controlled trial. Neurology. 2012; 79:785–792. [PubMed: 22843282]

23. Coelho T, Maia LF, da Silva AM, Cruz MW, Plante-Bordeneuve V, Suhr OB, Conceicao I, Schmidt HH, Trigo P, Kelly JW, Labaudiniere R, Chan J, Packman J, Grogan DR. Long-term effects of

tafamidis for the treatment of transthyretin familial amyloid polyneuropathy. J Neurol. 2013; 260:2802–2814. [PubMed: 23974642]

24. Berk JL, Suhr OB, Obici L, Sekijima Y, Zeldenrust SR, Yamashita T, Heneghan MA, Gorevic PD, Litchy WJ, Wiesman JF, Nordh E, Corato M, Lozza A, Cortese A, Robinson-Papp J, Colton T, Rybin DV, Bisbee AB, Ando Y, Ikeda S, Seldin DC, Merlini G, Skinner M, Kelly JW, Dyck PJ. Repurposing diflunisal for familial amyloid polyneuropathy: a randomized clinical trial. JAMA. 2013; 310:2658–2667. [PubMed: 24368466]
25. Waddington Cruz M, Amass L, Keohane D, Schwartz J, Li H, Gundapaneni B. Early intervention with tafamidis provides long-term (5.5-year) delay of neurologic progression in transthyretin hereditary amyloid polyneuropathy. Amyloid. 2016; 23:178–183. [PubMed: 27494299]
26. Haass C, Selkoe DJ. Soluble protein oligomers in neurodegeneration: lessons from the Alzheimer's amyloid beta-peptide. Nat Rev Mol Cell Biol. 2007; 8:101–112. [PubMed: 17245412]
27. Maurer MS, Grogan DR, Judge DP, Mundayat R, Packman J, Lombardo I, Quyyumi AA, Aarts J, Falk RH. Tafamidis in transthyretin amyloid cardiomyopathy: effects on transthyretin stabilization and clinical outcomes. Circ Heart Fail. 2015; 8:519–526. [PubMed: 25872787]
28. Castano A, Helmke S, Alvarez J, Delisle S, Maurer MS. Diflunisal for ATTR cardiac amyloidosis. Congest Heart Fail. 2012; 18:315–319. [PubMed: 22747647]
29. Ericzon BG, Wilczek HE, Larsson M, Wijayatunga P, Stangou A, Pena JR, Furtado E, Barroso E, Daniel J, Samuel D, Adam R, Karam V, Poterucha J, Lewis D, Ferraz-Neto BH, Cruz MW, Munar-Ques M, Fabregat J, Ikeda S, Ando Y, Heaton N, Otto G, Suhr O. Liver Transplantation for Hereditary Transthyretin Amyloidosis: After 20 Years Still the Best Therapeutic Alternative? Transplantation. 2015; 99:1847–1854. [PubMed: 26308415]
30. Kastritis E, Wechalekar AD, Dimopoulos MA, Merlini G, Hawkins PN, Perfetti V, Gillmore JD, Palladini G. Bortezomib with or without dexamethasone in primary systemic (light chain) amyloidosis. J Clin Oncol. 2010; 28:1031–1037. [PubMed: 20085941]
31. Lamm W, Willenbacher W, Lang A, Zojer N, Muldur E, Ludwig H, Schauer-Stalzer B, Zielinski CC, Drach J. Efficacy of the combination of bortezomib and dexamethasone in systemic AL amyloidosis. Annals Hematol. 2011; 90:201–206.
32. Reixach N, Deechongkit S, Jiang X, Kelly JW, Buxbaum JN. Tissue damage in the amyloidoses: Transthyretin monomers and nonnative oligomers are the major cytotoxic species in tissue culture. Proc Natl Acad Sci U S A. 2004; 101:2817–2822. [PubMed: 14981241]
33. Lashuel HA, Lai Z, Kelly JW. Characterization of the transthyretin acid denaturation pathways by analytical ultracentrifugation: implications for wild-type, V30M, and L55P amyloid fibril formation. Biochemistry. 1998; 37:17851–17864. [PubMed: 9922152]
34. Lashuel HA, Wurth C, Woo L, Kelly JW. The most pathogenic transthyretin variant, L55P, forms amyloid fibrils under acidic conditions and protofilaments under physiological conditions. Biochemistry. 1999; 38:13560–13573. [PubMed: 10521263]
35. Jiang X, Smith CS, Petrassi HM, Hammarstrom P, White JT, Sacchettini JC, Kelly JW. An engineered transthyretin monomer that is nonamyloidogenic, unless it is partially denatured. Biochemistry. 2001; 40:11442–11452. [PubMed: 11560492]
36. Bergstrom J, Gustavsson A, Hellman U, Sletten K, Murphy CL, Weiss DT, Solomon A, Olofsson BO, Westermark P. Amyloid deposits in transthyretin-derived amyloidosis: cleaved transthyretin is associated with distinct amyloid morphology. J Pathol. 2005; 206:224–232. [PubMed: 15810051]
37. Eisenberg D, Jucker M. The amyloid state of proteins in human diseases. Cell. 2012; 148:1188–1203. [PubMed: 22424229]
38. Tycko R. Amyloid Polymorphism: Structural Basis and Neurobiological Relevance. Neuron. 2015; 86:632–645. [PubMed: 25950632]
39. Azevedo EPC, Pereira HM, Garratt RC, Kelly JW, Foguel D, Palhano FL. Dissecting the structure, thermodynamic stability and aggregation properties of the A25T transthyretin (A25T-TTR) variant involved in leptomeningeal amyloidosis: identifying protein partners that co-aggregate during A25T-TTR fibrillogenesis in cerebrospinal fluid. Biochemistry. 2011; 50:11070–11083. [PubMed: 22091638]

40. Do Amaral B, Coelho T, Sousa A, Guimaraes A. Usefulness of labial salivary gland biopsy in familial amyloid polyneuropathy Portuguese type. Amyloid. 2009; 16:232–238. [PubMed: 19922336]
41. Niphakis MJ, Lum KM, Cognetta AB 3rd, Correia BE, Ichu TA, Olucha J, Brown SJ, Kundu S, Piscitelli F, Rosen H, Cravatt BF. A Global Map of Lipid-Binding Proteins and Their Ligandability in Cells. Cell. 2015; 161:1668–1680. [PubMed: 26091042]
42. Parker CG, Galmozzi A, Wang Y, Correia BE, Sasaki K, Joslyn CM, Kim AS, Cavallaro CL, Lawrence RM, Johnson SR, Narvaiza I, Saez E, Cravatt BF. Ligand and Target Discovery by Fragment-Based Screening in Human Cells. Cell. 2017; 168:527–541e529. [PubMed: 28111073]
43. Rostovtsev VV, Green LG, Fokin VV, Sharpless KB. A stepwise Huisgen cycloaddition process: Copper(I)-catalyzed regioselective "ligation" of azides and terminal alkynes. Angew Chem-Intl Ed. 2002; 41:2596.
44. Speers AE, Adam GC, Cravatt BF. Activity-based protein profiling in vivo using a copper(I)-catalyzed azide-alkyne 3+2 cycloaddition. J Am Chem Soc. 2003; 125:4686–4687. [PubMed: 12696868]
45. Dayon L, Hainard A, Licker V, Turck N, Kuhn K, Hochstrasser DF, Burkhard PR, Sanchez JC. Relative quantification of proteins in human cerebrospinal fluids by MS/MS using 6-plex isobaric tags. Anal Chem. 2008; 80:2921–2931. [PubMed: 18312001]
46. Suanprasert N, Berk JL, Benson MD, Dyck PJB, Klein CJ, Gollob JA, Bettencourt BR, Karsten V, Dyck PJ. Retrospective study of a TTR FAP cohort to modify NIS+7 for therapeutic trials. J Neurologic Sci. 2014; 344:121–128.
47. Arvidsson S, Pilebro B, Westermark P, Lindqvist P, Suhr OB. Amyloid Cardiomyopathy in Hereditary Transthyretin V30M Amyloidosis - Impact of Sex and Amyloid Fibril Composition. PLoS One. 2015; 10
48. Hu Y, Su B, Kim CS, Hernandez M, Rostagno A, Ghiso J, Kim JR. A strategy for designing a peptide probe for detection of beta-amyloid oligomers. Chembiochem. 2010; 11:2409–2418. [PubMed: 21031399]
49. Aoraha E, Candreva J, Kim JR. Engineering of a peptide probe for beta-amyloid aggregates. Mol Biosyst. 2015; 11:2281–2289. [PubMed: 26073444]
50. Reinke AA, Ung PM, Quintero JJ, Carlson HA, Gestwicki JE. Chemical probes that selectively recognize the earliest Abeta oligomers in complex mixtures. J Am Chem Soc. 2010; 132:17655–17657. [PubMed: 21105683]
51. Mangione PP, Porcari R, Gillmore JD, Pucci P, Monti M, Porcari M, Giorgetti S, Marchese L, Raimondi S, Serpell LC, Chen W, Relini A, Marcoux J, Clatworthy IR, Taylor GW, Tennent GA, Robinson CV, Hawkins PN, Stoppini M, Wood SP, Pepys MB, Bellotti V. Proteolytic cleavage of Ser52Pro variant transthyretin triggers its amyloid fibrillogenesis. Proc Natl Acad Sci U S A. 2014; 111:1539–1544. [PubMed: 24474780]
52. Marcoux J, Mangione PP, Porcari R, Degiacomi MT, Verona G, Taylor GW, Giorgetti S, Raimondi S, Sanglier-Cianferani S, Benesch JL, Cecconi C, Naqvi MM, Gillmore JD, Hawkins PN, Stoppini M, Robinson CV, Pepys MB, Bellotti V. A novel mechano-enzymatic cleavage mechanism underlies transthyretin amyloidogenesis. EMBO Mol Med. 2015; 7:1337–1349. [PubMed: 26286619]
53. Qiang W, Yau WM, Lu JX, Collinge J, Tycko R. Structural variation in amyloid-beta fibrils from Alzheimer's disease clinical subtypes. Nature. 2017
54. Sanders DW, Kaufman SK, DeVos SL, Sharma AM, Mirbaha H, Li A, Barker SJ, Foley AC, Thorpe JR, Serpell LC, Miller TM, Grinberg LT, Seeley WW, Diamond MI. Distinct tau prion strains propagate in cells and mice and define different tauopathies. Neuron. 2014; 82:1271–1288. [PubMed: 24857020]
55. Wang W, Hong S, Tran A, Jiang H, Triano R, Liu Y, Chen X, Wu P. Sulfated ligands for the copper(I)-catalyzed azide-alkyne cycloaddition. Chem Asian J. 2011; 6:2796–2802. [PubMed: 21905231]
56. Speers AE, Cravatt BF. Profiling enzyme activities in vivo using click chemistry methods. Chem Biol. 2004; 11:535–546. [PubMed: 15123248]

57. Plate L, Cooley CB, Chen JJ, Paxman RJ, Gallagher CM, Madoux F, Genereux JC, Dobbs W, Garza D, Spicer TP, Scampavia L, Brown SJ, Rosen H, Powers ET, Walter P, Hodder P, Wiseman RL, Kelly JW. Small molecule proteostasis regulators that reprogram the ER to reduce extracellular protein aggregation. Elife. 2016; 5

58. Benjamini Y, Krieger AM, Yekutieli D. Adaptive linear step-up procedures that control the false discovery rate. Biometrika. 2006; 93:491–507.

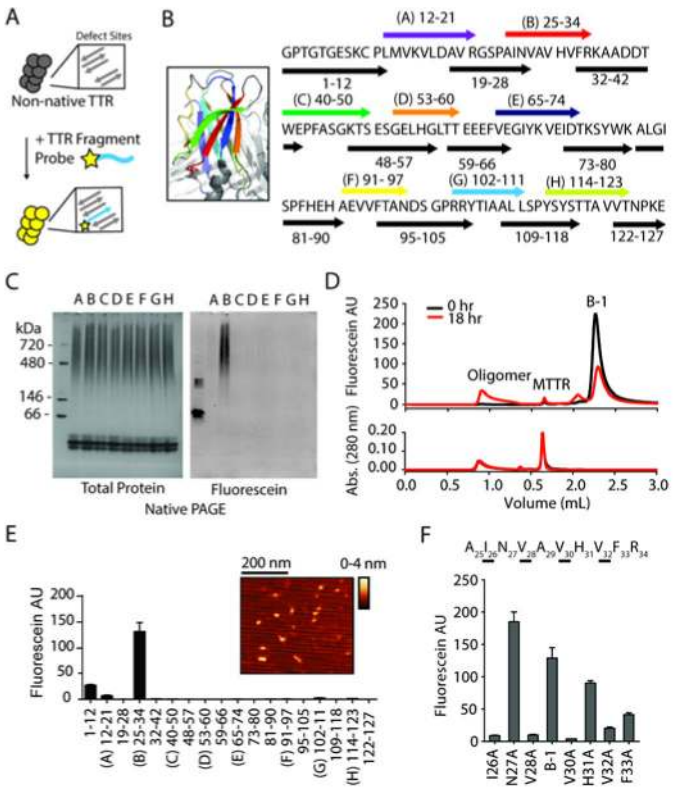

Fig. 1. The B β-strand of TTR labels non-native TTR oligomers

(**A**) Schematic diagrams illustrating our hypothesis that peptide fragments of TTR integrate into defect sites of TTR-derived oligomers to selectively label them. (**B**) TTR tetramer structure (Protein Data Bank I.D. = 4N85) and sequence, indicating the β-strands (in different colors, labeled from A to H) and segments between the β-strands (in black) that were each individually synthesized. Each peptide was fluorescently labeled at the N-terminus with fluorescein for detection. (**C**) Native PAGE of TTR strand derived peptides (A to H) incubated with MTTR oligomers. (**D**) SEC of probe B-1 incubated with MTTR oligomers. (**E**) Quantification of incorporation of each candidate TTR-derived peptide probe into MTTR oligomers using SEC. Inset: AFM image of the MTTR oligomers used in this peptide screen. (**F**) Effect of probe B-1 alanine mutations on incorporation into MTTR oligomers. The amino acids are numbered according to their position in the protein amino acid sequence. Error bars represent mean ± s.d. of at least three separate experiments.

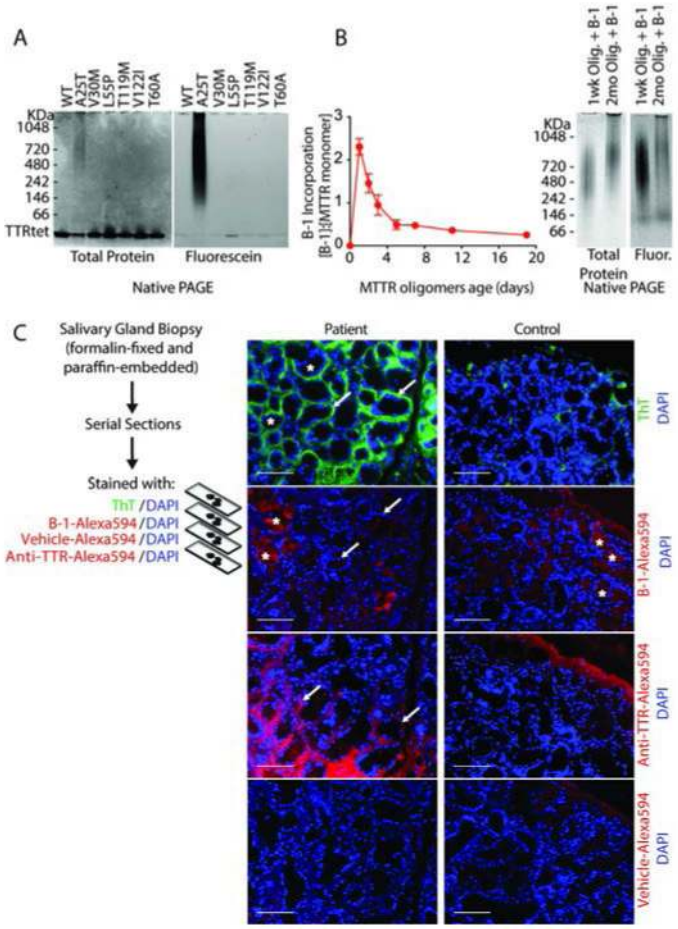

Fig. 2. Probe B-1 is selective for nascently formed soluble non-native oligomeric TTR

(**A**) Native PAGE of probe B-1 incubated with folded tetramers with the indicated mutations (TTR_{tet}) and A25T-derived aggregates. (**B**) Probe B-1 incorporation into MTTR oligomers as a function of oligomers' age measured by SEC. Error bars represent mean ± s.d. of at least three separate experiments. (Right) Native PAGE showing the molecular weight and labeling intensity differences between 1-week-old MTTR oligomers and 2-month-old MTTR oligomers. (**C**) Probe B-1-Biotin labeling of salivary gland biopsies of a FAP patient (n=2; left panel) and a non-FAP control (n=2; right panel). Arrows indicate regions with amyloid fibrils (around the glandular acini in the patient sample (40)), stained by thioflavin T (ThT; top row) and the anti-TTR antibody (anti-TTR-Alexa594; third row) not labeled by probe B-1-Biotin (B-1-Alexa594; second row). Asterisks indicate regions inside the glandular acini that are labeled by B-1-Biotin in both the patient and the control samples. Scale bars represent 1 mm in length.

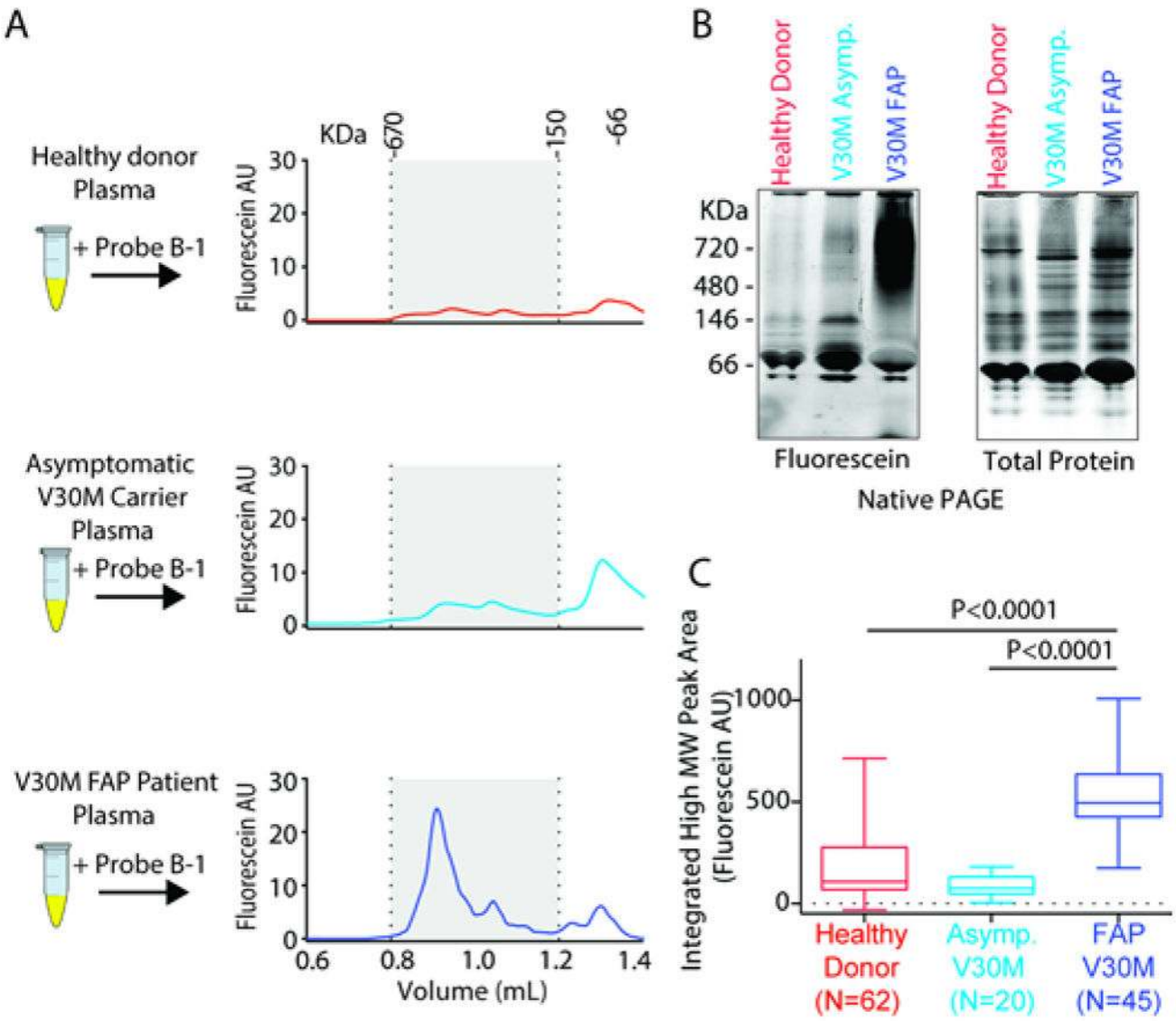

Fig. 3. Probe B-1 selectively differentiates FAP patient samples from controls

(**A**) Experimental set-up and representative SEC chromatograms where probe B-1 was incubated with the indicated samples for 24 h, before injection onto an SEC column. Probe B-1 selectively labels the high MW fraction (800–1200 μL, 150–660 kDa) in the V30M FAP patient sample. (**B**) Representative Native PAGE of the samples in panel **A**. (**C**) High MW peak area (150–660 kDa) of healthy donors (n=62, average age = 43 ± 11 (s.d.)), asymptomatic V30M carriers (n=20, average age = 34 ± 11(s.d.)), and V30M FAP patients (n=45, average age = 41 ± 14(s.d.)). Comparison by ANOVA followed by post-hoc analysis with Tukey correction for multiple pairwise comparisons.. Box plot whiskers represent the 2.5–97.5% range.

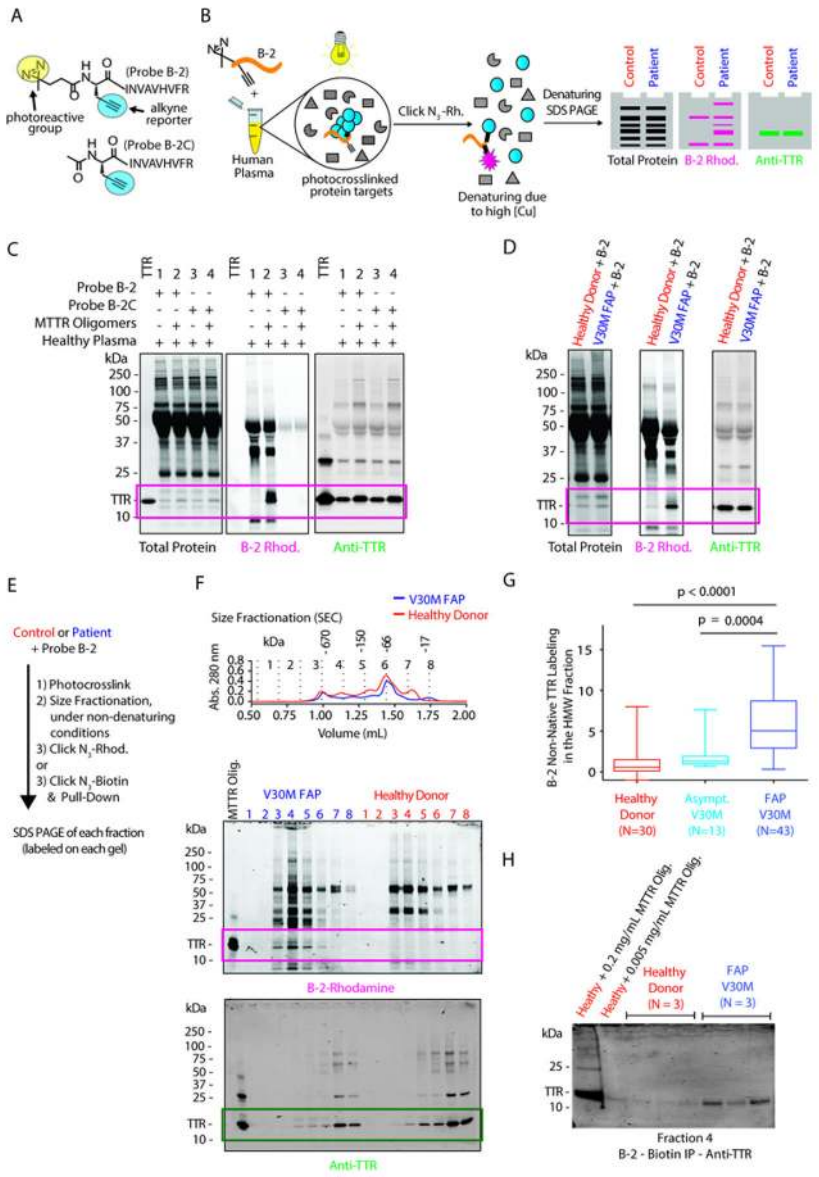

Fig. 4. Probe B-2 labels non-native TTR in patient plasma

(A) Chemical structure of probe B-2, containing a photoactivatable crosslinker (diazirine) and reporter (alkyne) functional group, and probe B-2C, lacking the diazirine. **(B)** Schematic of the photo-crosslinking approach used to generate panels (**C**) and (**D**), whereby B-2 is incubated with patient plasma, photo-crosslinked via the diazirine and then visualized by reducing SDS PAGE analysis after rhodamine conjugation to the alkyne handle. (**C**) SDS PAGE demonstrating probe B-2 selective and covalent labeling of recombinant MTTR oligomers that were added to healthy donor plasma. TTR labeling by probe B-2 is indicated by the magenta box. (**D**) SDS PAGE demonstrating that probe B-2 differentially covalently labels TTR in patient plasma, but not in control plasma. TTR labeling by probe B-2 is indicated by the magenta box. (**E**) Experimental set-up for panels (**F**), (**G**) and (**H**). After incubation and photo-crosslinking, each sample was fractionated by SEC before conjugation

of rhodamine or biotin to the alkyne handle. The high [Cu] in this reaction denatures the proteome, thus non-denaturing SEC is done first. (**F**) Top: representative SEC chromatogram of a patient and control plasma sample. Middle: reducing SDS PAGE of probe B2-rhodamine conjugated proteins, TTR labeling by B-2 is indicated by the magenta box. Bottom: anti-TTR immunoblot is indicated by the dark green box. (**G**) SDS-PAGE band densitometry quantification of probe B-2 TTR labeling in the high MW SEC fractions (fractions 3 & 4, see fig. S11 for experimental design schematic and additional representative data) from healthy donors (n=30), V30M asymptomatic mutation carriers (n=13), and V30M FAP patients (n=43). *P*-values were calculated by ANOVA test followed by post-hoc analysis with Tukey correction for multiple pairwise comparisons. Box plot whiskers represent the 2.5–97.5% range. **(H)** Biotin pulldown and anti-TTR immunoblot of probe B-2-conjugated proteins from the high MW fraction #4 in F.

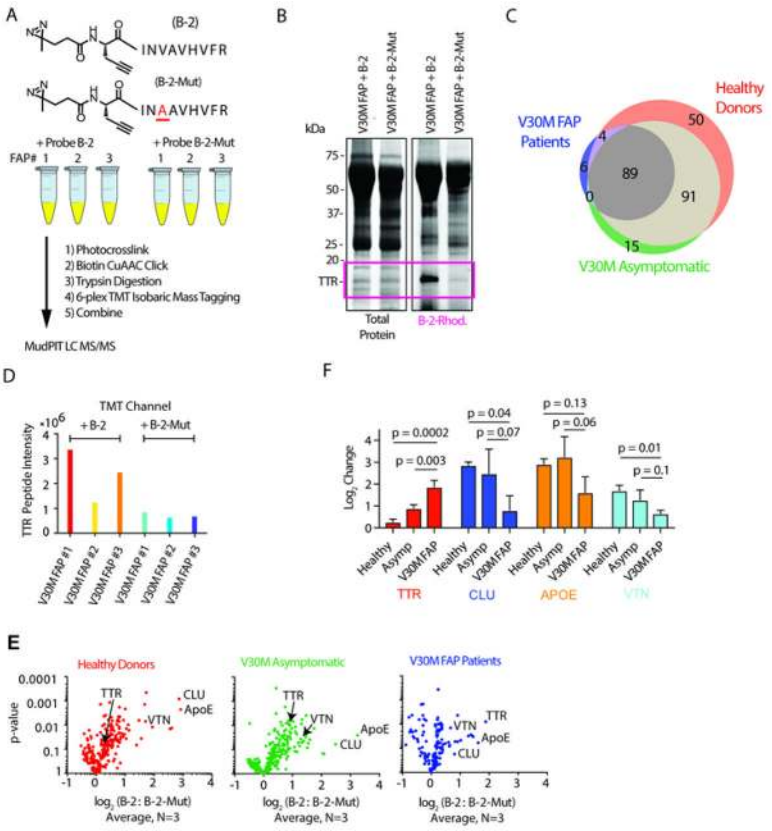

Fig. 5. Targeted mass spectrometry confirms non-native TTR as a target of the B-peptide

(**A**) Experimental scheme where either probe B-2 or a probe B-2 mutant (V28A or B-2-Mut) is incubated with either patient or control plasma. After photo-crosslinking, biotin is conjugated to the alkyne handle and the probe B-2–biotin conjugates enriched with streptavidin. After trypsin digestion, the trypsin fragments are labeled with one of six TMT tags, then combined and subjected to MudPIT LC MS/MS analysis. (**B**) Rhodamine fluorescence labeling of non-native TTR oligomers from a V30M FAP patient incubated with probe B-2 compared to probe B-2-Mut (magenta box). (**C**) Venn diagram showing the overlap of proteins identified from healthy blood donors, V30M asymptomatic mutation carriers, and V30M FAP patients. (**D**) Intensity of TTR peptide signal from plasma of three FAP patients treated with either probe B-2 or probe B-2-Mut. (**E**) Volcano plot of identified proteins quantified by TMT isobaric mass tags shown as a ratio of the intensity in the probe B-2 TMT channel to that of the corresponding probe B-2-Mut TMT channel. Enrichment ratios are shown as an average (n=3) and *P*-values were calculated from the $\log_2$ transformed values using a two tailed t-test assuming equal standard deviations followed by a correction for multiple testing using a FDR of 5% (table S1) as described in the Materials and Methods. **F**) Probe B-2 to probe B-2-Mut ratios for a select number of proteins previously identified in TTR amyloid deposits. *P*-values were calculated by an ANOVA test followed by post-hoc analysis with Tukey correction for multiple pairwise comparisons. *P*-values were calculated using a two-tailed t-test.

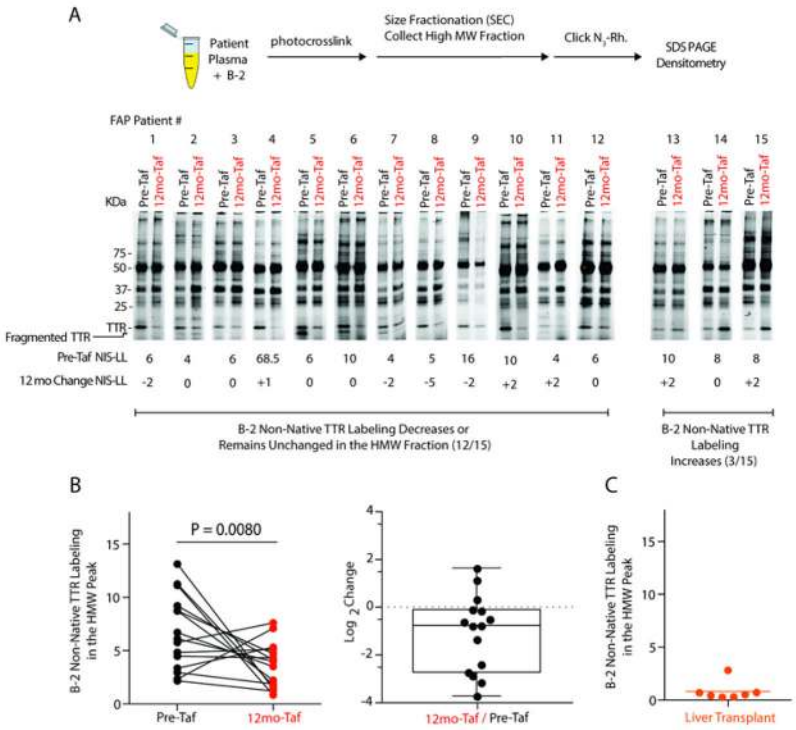

Fig. 6. Labeling of high molecular weight non-native TTR oligomers decreases in V30M FAP patients treated with tafamidis or liver transplantation

(**A**) (Top) Schematic representing the experimental workflow. (Bottom) Representative probe B-2 rhodamine gel images from the high MW SEC fraction from 15 Portuguese FAP patients whose blood was taken prior to treatment and after 12 months treatment with the kinetic stabilizer tafamidis. The NIS-LL score for each patient and the change after 12 months is listed below each gel. **(B)** Quantification of probe B-2 non-native TTR labeling by band densitometry (left) and fold change after 12 months of treatment (right). *P*-value was calculated by a two-tailed unpaired t-test comparing the pre-tafamidis and 12 mo time points. Box plot whiskers represent the min-max. (C) Non-native TTR labeling by B-2 of 7 V30M FAP patients (Japan) whom underwent liver transplantation (0.8 ± 0.3; mean ± s.d.).

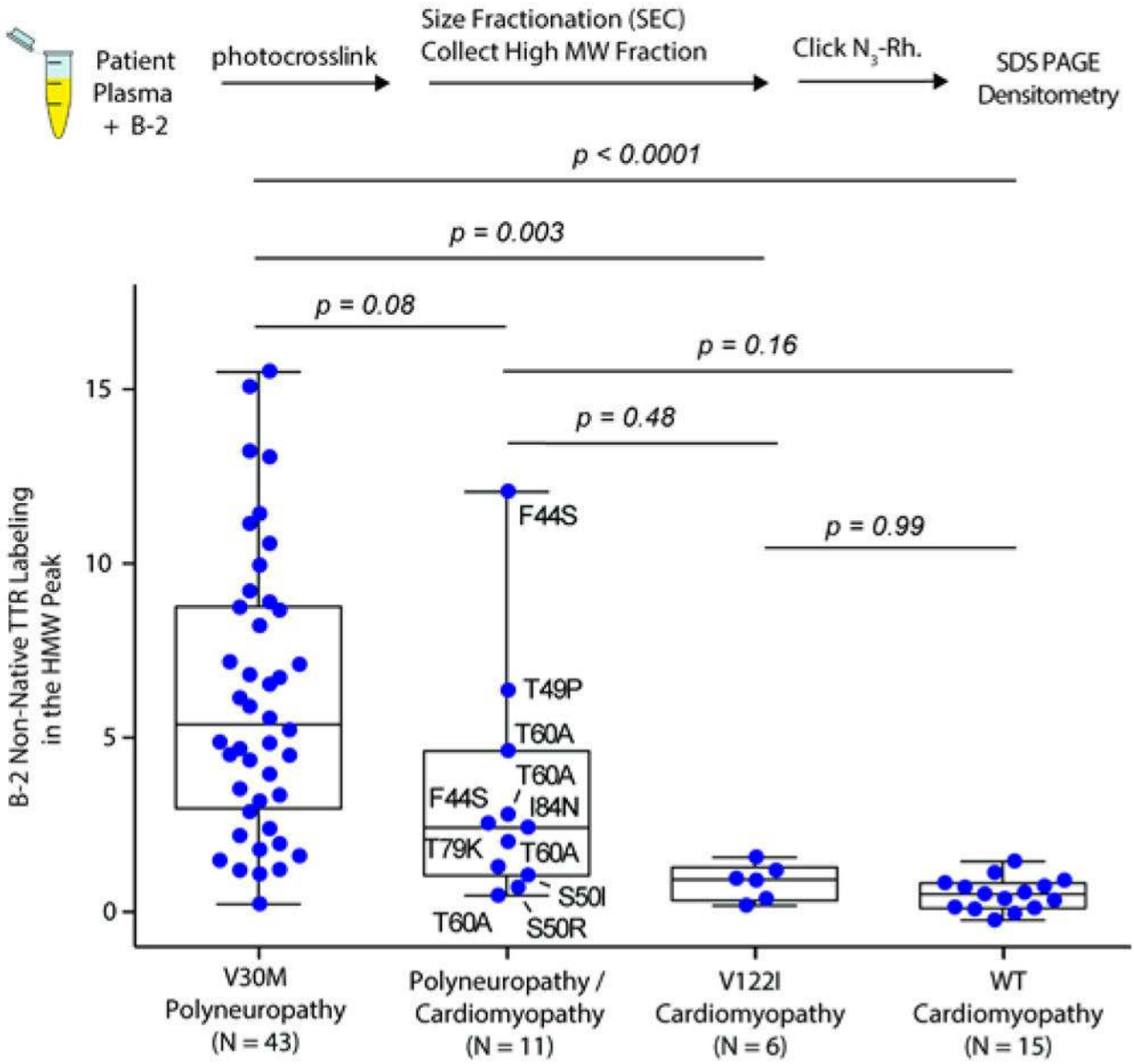

Fig. 7. Non-native TTR is detected in predominantly neuropathic hereditary TTR amyloidosis and not detected in cardiomyopathy-associated genotypes

(Top) Experimental schematic. (Bottom) Non-native TTR expression in TTR amyloidosis genotypes other than V30M (individual mutations as indicated) as detected by B-2 photocrosslinking and SDS-PAGE. The y-axis refers to values calculated by gel densitometry. *P*-values were calculated using an ANOVA test followed by post-hoc analysis with Tukey correction for multiple pairwise comparisons. V30M FAP data from Fig. 4G is presented for comparison. Box plot whiskers represent the 2.5–97.5% range.

Table 1

Sample age and demographics for the non-native TTR detection by the B-2 SDS PAGE assay presented in Fig. 4H, Fig. 6, and Fig. 7.

Genotype (n)	Female/Male	Age (Mean ± s.d.)	Origin
Healthy Donors (30)	18/12	51 ± 16	US (28), Japan (2)
V30M Asymptomatic (13)	6/7	36 ± 13	Portugal (12), US (1)
V30M FAP (43)	21/22	43 ± 14	Portugal (34), Japan (7), US (2)
WT Cardiomyopathy (15)	1/14	76 ± 8	US (15)
V122I (6)	4/2	76 ± 8	US (6)
Other: T60A (4), F44S (2), T79K (1), T49P (1), I84N (1), S50I (1), S50R (1),	5/6	56 ± 11	US (6), Japan (5)